

Accepted Manuscript

Singlet-triplet interaction in Group 2 M_2O hypermetallic oxides

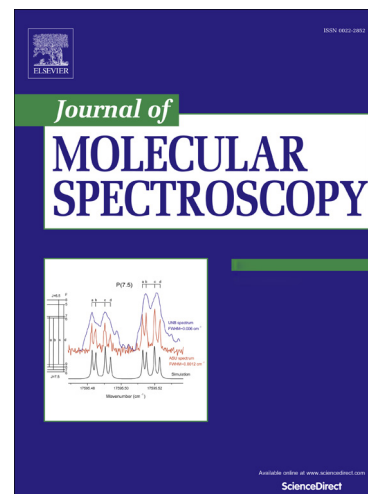
B. Ostojić, Per Jensen, P. Schwerdtfeger, P.R. Bunker

PII: S0022-2852(14)00103-9

DOI: <http://dx.doi.org/10.1016/j.jms.2014.05.003>

Reference: YJMSP 10442

To appear in: *Journal of Molecular Spectroscopy*



Please cite this article as: B. Ostojić, P. Jensen, P. Schwerdtfeger, P.R. Bunker, Singlet-triplet interaction in Group 2 M_2O hypermetallic oxides, *Journal of Molecular Spectroscopy* (2014), doi: <http://dx.doi.org/10.1016/j.jms.2014.05.003>

This is a PDF file of an unedited manuscript that has been accepted for publication. As a service to our customers we are providing this early version of the manuscript. The manuscript will undergo copyediting, typesetting, and review of the resulting proof before it is published in its final form. Please note that during the production process errors may be discovered which could affect the content, and all legal disclaimers that apply to the journal pertain.

Singlet-triplet interaction in Group 2 M_2O hypermetallic oxides

B. Ostojić,^a Per Jensen,^b P. Schwerdtfeger,^c
and P. R. Bunker^{1, c}

^a*Institute of Chemistry, Technology and Metallurgy, University of Belgrade,
Studentski trg 14-16, 11 000 Belgrade, Serbia*

^b*FB C – Physikalische und Theoretische Chemie, Bergische Universität,
D-42097 Wuppertal, Germany*

^c*Centre for Theoretical Chemistry and Physics (CTCP), The New Zealand
Institute for Advanced Study (NZIAS), Massey University Auckland, Private Bag
102904, 0745 Auckland, New Zealand*

Abstract

This *ab initio* study of Group 2 M_2O hypermetallic oxides focuses mainly on the two heaviest members, Ba_2O and Ra_2O . In accordance with previous studies in our group on the Be, Mg, Ca and Sr hypermetallic oxides, we find that the $BaOBa$ and $RaORa$ molecules have a linear $\tilde{X}^1\Sigma_g^+$ ground electronic state and a very low lying first excited $\tilde{a}^3\Sigma_u^+$ triplet electronic state. Special attention is placed on calculating and understanding how the singlet-triplet splitting and singlet-triplet interaction strength vary down the series. The calculations reveal that $MgOMg$ shows the largest singlet-triplet splitting and does not fit into the overall trend down the Group 2 series of elements. However, in all cases the extent of the singlet-triplet interaction between vibronic levels of the \tilde{X} and \tilde{a} states is very small. On the experimental side, there is literature evidence for the formation of electronically excited Ba_2O in oxidation reactions of Barium dimers, and our calculations of excited singlet and triplet state energies support that assignment.

Keywords : $BaOBa$, $RaORa$, *ab initio* 3D potential energy surfaces, rovibronic spectra, singlet-triplet interaction, hypermetallicity

¹ Permanent address: Steacie Laboratory, National Research Council of Canada, Ottawa, Ontario K1A0R6, Canada

1 INTRODUCTION

This paper reports the results of *ab initio* calculations that predict the geometry and electron spin multiplicity of the lowest two electronic states of the Ba_2O and Ra_2O molecules. The calculations are a continuation of our systematic studies of the alkaline earth hypermetallic oxides Be_2O [1], Mg_2O [2], Ca_2O [3], and Sr_2O [4]. For all six of these MOM molecules we find that the ground electronic state is a linear symmetric singlet state ($\tilde{X}^1\Sigma_g^+$), and that there is a low lying linear symmetric triplet state ($\tilde{a}^3\Sigma_u^+$) close by. Here we focus particularly on calculating and understanding the variation of the singlet-triplet splitting, and singlet-triplet interaction, in this series of six molecules.

There are many reasons for studying Group 2 M_2O molecules. Our primary interest is in their electronic structure, since they are examples of molecules having metal stoichiometries that exceed normal valence. We are also interested in the fact they exhibit a very small singlet-triplet splitting, and wonder whether, for the heaviest members of the series, singlet-triplet interaction perturbations could provide indicators for determining the possible time-dependence of the electron-to-proton mass ratio m_e/M_p and of the fine-structure constant α [5–7]. In more down to earth terms, the study of metal-rich clusters, both by *ab initio* calculation and by spectroscopic investigation, is important particularly in the light of developing new catalytic materials. Moreover, the study of small clusters can help in understanding the emergence of crystalline properties from molecular properties.

Of course, such theoretical results as ours must be supported by spectroscopic studies. Chemiluminescence in the region 640–900 nm was produced in oxidation reactions of barium dimers and assigned as being due to the Ba_2O molecule [8–10]. The results of our calculations support this assignment, and we encourage further work examining the spectra of these Group 2 molecules based on the results of our calculations. At the Kernfysisch Versneller Instituut (KVI) of the University of Groningen, isotopes of radium are routinely produced and used in spectroscopy experiments [11,12]; studies of Ra_2O are therefore feasible.

2 AB INITIO CALCULATIONS OF THE SINGLET-TRIPLET SPACING IN M_2O OXIDES

We have computed the energies of the \tilde{X} and \tilde{a} electronic states of BaOBa and RaORa by employing the complete active space (CASSCF) technique [13,14], followed by a multi-reference configuration interaction (MRCI) treatment [15–17]. Our calculations show that both BaOBa and RaORa have a $\tilde{X}^1\Sigma_g^+$ ground

electronic state and a very low lying $\tilde{a}^3\Sigma_u^+$ first excited electronic state. In accord with our earlier studies of the Be, Mg, Ca and Sr hypermetallic oxides [1–4], the description of the $\tilde{X}^1\Sigma_g^+$ ground electronic state requires a multiconfigurational approach [18]. In contrast, the triplet state is well described by a single reference wavefunction. The singlet-triplet splittings are all in the region of 300 to 700 cm^{-1} due to the well separated electron spins on both metal atoms.

For BaOBa, the CASSCF calculations show that the two most important configurations for the $\tilde{X}^1\Sigma_g^+$ ground state are $|\dots 10\sigma_u^2 11\sigma_g^2 12\sigma_g^2 13\sigma_g^2 6\pi_g^4 11\sigma_u^2 6\pi_u^4 7\pi_u^4 12\sigma_u^2 14\sigma_g^2 \rangle$ and $|\dots 12\sigma_u^2 13\sigma_u^2 \rangle$. On the other hand, the $\tilde{a}^3\Sigma_u^+$ state is well described by the single-reference wave function: $|\dots 14\sigma_g^1 13\sigma_u^1 \rangle$. The $10\sigma_u$ and $11\sigma_g$ molecular orbitals are mainly antisymmetric and symmetric linear combinations, respectively, of the Ba 5s atomic orbitals. The $12\sigma_g$ orbital consists mainly of the O 2s orbital. The $12\sigma_u$ orbital is mainly the O $2p_z$ orbital directed along the internuclear z -axis. The $7\pi_u$ orbital consists mainly of the O $2p_{x,y}$ orbitals. The molecular orbitals that involve linear combinations of the Ba 5p orbitals (i.e., $13\sigma_g$, $6\pi_g$, $11\sigma_u$, and $6\pi_u$) are placed energetically between the $12\sigma_g$ and two higher-lying orbitals $7\pi_u$ and $12\sigma_u$, which is different from the ordering of the molecular orbitals in MgOMg and CaOCa, but similar to the ordering of the orbitals in SrOSr. The $11\sigma_u$ and $13\sigma_g$ orbitals are mainly composed of antisymmetric and symmetric linear combinations, respectively, of the Ba $5p_z$ orbitals. The $6\pi_u$ and $6\pi_g$ orbitals are mainly symmetric and antisymmetric linear combinations, respectively, of the Ba $5p_{x,y}$ orbitals. The highest occupied molecular orbitals are the $14\sigma_g$ and $13\sigma_u$ orbitals; they are mainly symmetric and antisymmetric linear combinations, respectively, of the Ba 6s orbitals.

From the CASSCF calculations for RaORa, we find that the most important configurations for the ground electronic state are, $|\dots 14\sigma_u^2 15\sigma_g^2 16\sigma_g^2 15\sigma_u^2 9\pi_g^4 9\pi_u^4 17\sigma_g^2 16\sigma_u^2 10\pi_u^4 18\sigma_g^2 \rangle$ and $|\dots 10\pi_u^4 17\sigma_u^2 \rangle$. However, the $\tilde{a}^3\Sigma_u^+$ state of RaORa is well described by the single-reference wave function: $|\dots 18\sigma_g^1 17\sigma_u^1 \rangle$. The $14\sigma_u$ and $15\sigma_g$ orbitals are mainly antisymmetric and symmetric linear combinations, respectively, of the Ra 6s orbitals. The $16\sigma_g$ orbital consists mainly of the O 2s orbital. The $16\sigma_u$ orbital consists mainly of the O $2p_z$ orbital. The $10\pi_u$ orbital consists mainly of the O $2p_{x,y}$ orbitals. The molecular orbitals that involve linear combinations of the Ra 6p orbitals ($15\sigma_u$, $9\pi_g$, $9\pi_u$, and $17\sigma_g$) are placed energetically between the $16\sigma_g$ and two higher-lying orbitals, $16\sigma_u$ and $10\pi_u$, which is similar to the ordering of the orbitals in BaOBa. The $15\sigma_u$ and $17\sigma_g$ orbitals are mainly composed of antisymmetric and symmetric linear combinations, respectively, of Ra $6p_z$ orbitals. The $9\pi_u$ and $9\pi_g$ orbitals are mainly symmetric and antisymmetric linear combinations, respectively, of the Ra $6p_{x,y}$ orbitals. The highest occupied molecular orbitals are the $18\sigma_g$ and $17\sigma_u$ orbitals; they are mainly symmetric and antisymmetric linear combinations, respectively, of Ra 7s orbitals.

2.1 Equilibrium geometries

For the geometry optimization of the \tilde{X} and \tilde{a} electronic states of BaOBa and RaORa we employed the cc-pCVQZ atomic orbital basis set for oxygen. Barium and radium are heavy elements and relativistic effects are significant; for them we used a Stuttgart small-core relativistic effective core potential, ECP46MDF [19] and ECP78MDF [19], respectively, together with the corresponding optimized valence basis set [19].

We chose a CASSCF active space consisting of all configurations obtained by distributing the 26 electrons ($2s^22p^4$ on O and $5s^25p^66s^2$ on each Ba) in 14 MOs of BaOBa ($11-14\sigma_g$, $10-13\sigma_u$, $6-7\pi_u$, and $6\pi_g$) and the 26 electrons ($2s^22p^4$ on O and $6s^26p^67s^2$ on each Ra) in 14 MOs ($15-18\sigma_g$, $14-17\sigma_u$, $9-10\pi_u$, and $9\pi_g$) of RaORa. Using the C_{2v} point group, the active space consists of six orbitals of A_1 symmetry, two of B_1 symmetry, five of B_2 symmetry, and one of A_2 symmetry. For the singlet and triplet electronic states we used the CASSCF state averaging (SA) procedure, i.e. 1^1A_1 and 1^3B_2 in the C_{2v} group and the two states were included with equal weights. The CI expansion of the CASSCF wavefunction starting from the CAS(26,14) orbitals was generated within the internally contracted method using single and double substitutions (MRCISD) from each reference determinant in a full space of active virtual orbitals. In these MRCISD calculations all 26 valence electrons were correlated and the effect of higher excitations were taken into account by using the Davidson correction [20]. All electronic structure calculations were carried out using the MOLPRO 2010.1 suite of programs [21]. We find that both \tilde{X} and \tilde{a} states of BaOBa are linear with an equilibrium Ba-O bond length of 2.201 Å. The \tilde{X} and \tilde{a} states of RaORa also have a linear equilibrium geometry with Ra-O bond lengths of 2.280 Å and 2.289 Å, respectively.

2.2 Singlet-triplet spacing

An interesting aspect of the theoretical study of these Group 2 hypermetallic oxides is the relatively small spacing between the singlet and the triplet states. For consistency and because of the small the singlet-triplet splittings, for the calculations of this splitting between the \tilde{X} and \tilde{a} electronic states of BeOBe, MgOMg, CaOCa, SrOSr, BaOBa and RaORa we employed an all-electron approach. Here the basis set for the oxygen atom was the cc-pCVQZ basis set. For the Be atom we used the Sapporo-TZP-2012 and Sapporo-QZP-2012 basis sets with the addition of extra s and p diffuse functions. For the Mg atom we used natural orbital based segmented contracted Gaussian type functions calculated using the 3rd order Douglas-Kroll-Hess approximation (DKH3-Gen-TK+NOSeC-CV-TZP and DKH3-Gen-TK+NOSeC-CV-QZP) with the ad-

dition of s and p diffuse functions. For the Ca, Sr and Ba atoms we used the corresponding Sapporo-TZP-2012 and Sapporo-QZP-2012 basis sets with the addition of s and p diffuse functions, whereas for the Ra atom we used the DKH3-Gen-TK+NOSec-CV-TZP and DKH3-Gen-TK+NOSec-CV-QZP basis sets with the addition of s and p diffuse functions. The basis sets were extracted from the Sapporo Data Base of Segmented Gaussian Basis Sets [22].

The 10 valence electrons ($2s^22p^4$ on O, and $2s^2, 3s^2, 4s^2, 5s^2, 6s^2$ or $7s^2$ on each metal) can be distributed in 12 MOs. The active space for the CASSCF calculations of BeOBe and MgOMg therefore included this full-valence space. However, the accurate description of the ground electronic state and the first triplet electronic state of CaOCa, SrOSr, BaOBa, and RaORa requires the correlation (polarization) of the core electrons. On the other hand, valence antibonding orbitals also need to be taken into account. To expand the active space, the energies of the \tilde{X} and \tilde{a} electronic states were computed by employing the CASSCF technique followed by a MRCI treatment and a modified version of CASPT2 (Complete Active Space with Second-order Perturbation Theory) developed by Celani and Werner [23], referred to as RS2C.

The inactive space in the CASSCF calculations of CaOCa consisted of the $1-5\sigma_g, 1-4\sigma_u, 1\pi_u,$ and $1-2\pi_g$ orbitals, whereas the active space involved $6-9\sigma_g, 5-8\sigma_u,$ and $2-4\pi_u$. The inactive space for the CASSCF calculations of SrOSr contained $1-8\sigma_g, 1-7\sigma_u, 1-3\pi_u, 1-4\pi_g, 1\delta_g,$ and $1\delta_u,$ and the active space involved $9-12\sigma_g, 4-6\pi_u,$ and $8-11\sigma_u$. The inactive space for the CASSCF calculations of BaOBa involved $1-11\sigma_g, 1-10\sigma_u, 1-5\pi_u, 1-6\pi_g, 1-2\delta_g,$ and $1-2\delta_u,$ and the active space involved $12-15\sigma_g, 6-8\pi_u,$ and $13-16\sigma_u$. The active space in the CASSCF calculations of CaOCa, SrOSr, and BaOBa consisted of all configurations obtained by distributing the 18 electrons in 14 MOs. The closed-shell orbitals for the CASSCF calculations of RaORa were $1-15\sigma_g, 1-15\sigma_u, 1-8\pi_u, 1-9\pi_g, 1-4\delta_g, 1-4\delta_u, 1\phi_u,$ and $1\phi_u$ while the orbitals $16-19\sigma_g, 16-18\sigma_u,$ and $9-11\pi_u$ formed the active space. The active space in the CASSCF calculations of RaORa consisted of all configurations obtained by distributing the 16 electrons in 13 MOs. The singlet and triplet electronic states were averaged in the state averaging (SA) CASSCF procedure and the two states were included with equal weights.

The CI expansion of the CASSCF wave function starting from the CAS(18,14) orbitals for CaOCa, SrOSr and BaOBa, and CAS(16,13) for RaORa was generated within the internally contracted method with single and double substitutions (MRCISD) from each reference determinant. In these MRCISD calculations all 18 electrons for CaOCa, SrOSr and BaOBa and 16 electrons for RaORa were correlated and the effect of higher excitations were taken into account by using the Davidson correction as described above [20].

Two types of RS2C calculation were performed using the CAS(18,14) wave-

functions for CaOCa, SrOSr, and BaOBa, and using the CAS(16,13) wavefunctions for RaORa as references in the RS2C calculations. In the first type of calculation (hereafter designated $E_{\text{RS2C}}^{(1)}$) for CaOCa, SrOSr, BaOBa and RaORa the valence antibonding orbitals of π_g symmetry were also correlated in the RS2C approach. In the second type of calculation (hereafter denoted $E_{\text{RS2C}}^{(2)}$), the above mentioned orbitals were kept frozen in the RS2C approach. To avoid intruder state problems we applied an energy shift of 0.1 hartree, and energies obtained in the RS2C calculations were corrected for this shift. The energy values for the construction of the potential energy surfaces were obtained using the following expression:

$$E = E_{\text{MRCI}} + E_{\text{RS2C}}^{(1)} - E_{\text{RS2C}}^{(2)} \quad (1)$$

Scalar relativistic effects were taken into account by applying the second-order Douglas–Kroll–Hess Hamiltonian (DKH) [24–26] as incorporated in the MOLPRO 2010.1 program package.

A two-point extrapolation scheme [27,28] was employed in order to obtain the complete basis set (CBS) extrapolated value of the singlet-triplet energy spacing

$$E_X = E_{\text{CBS}} + AX^{-3} \quad (2)$$

where E_X is the energy obtained using a basis set with the cardinal number X , in our case abbreviated as E_{TZ} (for triple-zeta with $X = 3$) or E_{QZ} (for quadruple-zeta with $X = 4$). The E_{CBS} value is the basis set limit value of the energy. Two separate energy calculations were performed using the smaller (TZ) and the larger basis set (QZ) and the values obtained for the singlet-triplet spacings are given in Table 1.

The variation of the E_{CBS} values for the singlet-triplet splitting is presented in Figure 1. It shows that the MgOMg value is anomalous. Improvements in the basis sets, and the use of different Hamiltonians to account for relativistic effects, did not change the trend seen here. The bond distances increase in a natural way down the Group 2 MOM series, and the ionisation potentials for the neutral or positively charged metals decrease down the series from Be to Ra.[29,30] Thus all trends are smooth within this series with the exception that the ^2D excited state of Ca^+ and the heavier ions lies below the ^2P state.[29] We cannot explain the MgOMg anomaly in the singlet-triplet splitting.

Table 1

The singlet-triplet spacing E (in cm^{-1}) of the \tilde{X} and \tilde{a} electronic states for the Group 2 M-O-M molecules for the smaller (TZ) and larger (QZ) basis sets, and the CBS value. We also tabulate the ground state equilibrium bond lengths and the spin-orbit coupling matrix elements $\langle \Psi_{\text{elec}}^{(\tilde{a})} | \hat{H}_{\text{SO}} | \Psi_{\text{elec}}^{(\tilde{X})} \rangle_{\text{el}}$ (in cm^{-1}) calculated for MOM angles of 180° and 140° . See text for details.

	$r_e^{\tilde{X}}/\text{\AA}$	E_{TZ}	E_{QZ}	E_{CBS}	$\langle \Psi_{\text{elec}}^{(\tilde{a})} \hat{H}_{\text{SO}} \Psi_{\text{elec}}^{(\tilde{X})} \rangle_{\text{el}}$	
					180°	140°
BeOBe	1.409	321	297	280	0.002	0.2
MgOMg	1.801	655	655	656	0.007	0.7
CaOCa	1.995	324	314	307	0.002	0.4
SrOSr	2.150	301	326	344	0.006	1.9
BaOBa	2.201	534	520	510	0.064	11.7
RaORa	2.280	580	592	601	0.265	51.6

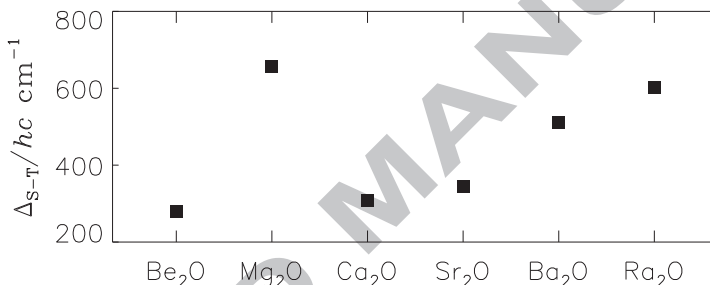


Fig. 1. The singlet-triplet splittings (E_{CBS} in Table 1) for the Group 2 M-O-M molecules.

2.3 Spin-orbit coupling

We have performed *ab-initio* calculations of the spin-orbit coupling matrix element as such effects become important for the heavier elements. We determined the *ab-initio* value of the one-electron integral $\langle \Psi_{\text{elec}}^{(\tilde{a})} | \hat{H}_{\text{SO}} | \Psi_{\text{elec}}^{(\tilde{X})} \rangle_{\text{el}}$, where $\Psi_{\text{elec}}^{(\tilde{X})}$ and $\Psi_{\text{elec}}^{(\tilde{a})}$ are the electronic wavefunctions using an all-electron spin-orbit operator that employs the second-order Douglas-Kroll-Hess (DKH) Hamiltonian as incorporated in the MOLPRO 2010.1 program package. Here \tilde{X} and \tilde{a} describes the two electronic states used, and the subscript ‘el’ indicates that integration is taken over electronic coordinates only. Note that the wave function needs to be accurately described in the core region as the all-electron spin-orbit operator acts on the core-part of the valence orbitals undergoing spin-orbit splitting. The value of this integral also is sensitive to the M-O-M bending angle, and it was therefore also determined at an M-O-M bending angle of 140° using the equilibrium M-O bond length of the linear

molecule (Table 1). This increase in spin-orbit contribution can be attributed to the different admixture of the vacant spin-orbit split p-levels of the Group 2 metals upon bending away from the linear geometry. Note however that there is little change in the spin densities on the metal atom upon bending. As shown in detail in our paper on SrOSr [4] (see, in particular, Fig. 3 and Table 6 in that paper), the singlet-triplet splitting is large in comparison to the vibronic singlet-triplet matrix elements, and so the extent of the singlet-triplet interaction between the vibronic states is very small.

3 THE ELECTRONIC SPECTRUM OF BaOBa

West and Poland [8] observed a broad banded chemiluminescence extending from 500 to 1150 nm by reacting Ba with CO₂ or CO in a heat pipe. This flame spectrum has a continuum-like appearance with several broad features, the most prominent of which occurs near 850 nm. As they state in their paper, the appearance of this flame spectrum does not allow the emitting species to be identified. However, they point out that irregularities in the spectrum suggest that both diatomic and polyatomic species are implicated. A short time later in 1977, Edelstein et al. [9] published an account of their study of the spatially resolved chemiluminescence of the Ba + O₂ reaction and suggested that the red part of the broad banded emission seen might be due Ba₂O. More recently, Gee et al. [10] have studied the emission spectra generated by the reaction of Ba₂ with N₂O on N₂ clusters, and of Ba₂ with CO₂ on Ar clusters. From this work they have been able to assign unambiguously part of the fluorescence emission observed in the work of West and Poland as being due to the Ba₂O molecule. The Ba₂O emission spectrum extends from 650 to 900 nm and consists of two broad bands: One centered at around 720 nm and the other, a narrower and more intense feature, centred at around 850 nm with a rather sharp cut-off at 900 nm.

We have calculated the low-lying BaOBa excited electronic singlet and triplet state energies in order to see if they support this assignment. Here we have used the CAS(8,10)-MRCISD+Q method, with the Sapporo-DZP-2012 basis set for Ba and the cc-pVTZ basis set for O, to calculate the equilibrium structures and energies. We have also calculated the bending potential curves of the low lying states, and these are shown in Fig.2. At linearity, the $\tilde{b}^3\Pi_u$ state is a Renner degenerate state. The equilibrium structures and the vertical absorption and emission energies are given in Tables 2 and 3. For both the singlet and triplet excited states the lowest excited states are bent at equilibrium. Our results clearly show that the broad band centred around 720 nm is triplet emission, whereas the 850 nm band is singlet emission. The broadness of each of the emission band systems is due to the presence of bending progressions that result from the large change in equilibrium bond angle between the upper

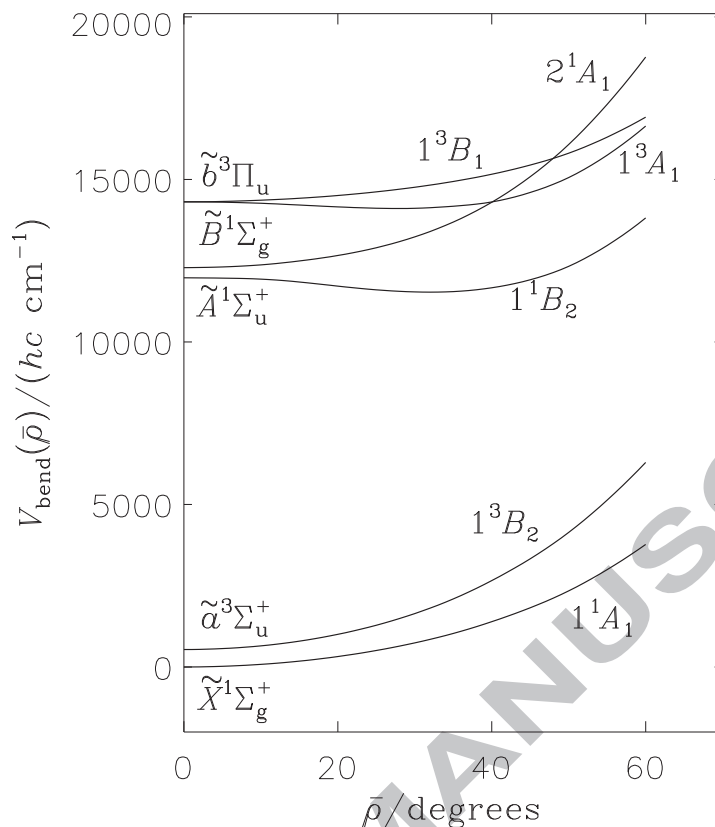


Fig. 2. The bending potential curves for the ground and low lying excited states of BaOBa.

and lower states. This supports very nicely the assignment of the emission as being due to BaOBa. Moreover, the electronic configuration of the $\tilde{b}^3\Pi_u$ state differs significantly in nature from the ground state. While the ground state can be approximately described as $Ba^+O^{2-}Ba^+$ with the two single electrons (radicals) being located at the two metal centres, the excited $^3\Pi_u$ state is a charge transfer state best described as $Ba^{0.5+}O^-Ba^{0.5+}$ with an electron being transferred from a σ_u into a π_u orbital, the latter consisting almost exclusively of a $p(O)$ -orbital. It is clear that the dipole moment for the bent structure changes from the ground state to the excited state in such a charge transfer process.

In conclusion, we have now completed our study of the Group 2 series of M_2O hypermetallic oxides from $M=Be$ to $M=Ra$. Each molecule has a linear symmetric $\tilde{X}^1\Sigma_g^+$ ground electronic state and a very low lying first excited $\tilde{a}^3\Sigma_u^+$ triplet electronic state; we have found that the extent of the spin-orbit coupling between the vibronic levels of these states is small. In the present paper we have focussed on the Ba and Ra molecules, and the nature of the broad 720 nm emission in Ba_2O has been identified as originating from a bent charge-transfer triplet state.

Table 2

Vertical singlet and triplet excitation energies ΔE_{vert} (in cm^{-1}) of the lowest singlet and triplet excited states of BaOBa, calculated at the state-average CAS-MRCISD+ Q level of theory. The calculations were carried out at the ground state equilibrium geometry of $\angle(\text{BaOBa}) = 180^\circ$ and $r(\text{Ba-O}) = 2.201 \text{ \AA}$.

Singlet states				
State Φ^a	ΔE_{vert}^b	$ \langle \Phi \mu_x \tilde{X} \rangle ^c$	$ \langle \Phi \mu_y \tilde{X} \rangle ^c$	$ \langle \Phi \mu_z \tilde{X} \rangle ^c$
$\tilde{X}^1\Sigma_g^+$ 1^1A_1	0	0.0	0.0	0.0
$\tilde{A}^1\Sigma_u^+$ 1^1B_2	11879	0.0	2.72	0.0
$\tilde{B}^1\Sigma_g^+$ 2^1A_1	12363	0.0	0.0	0.0
Triplet states				
State Φ^a	ΔE_{vert}^b	$ \langle \Phi \mu_x \tilde{a} \rangle ^c$	$ \langle \Phi \mu_y \tilde{a} \rangle ^c$	$ \langle \Phi \mu_z \tilde{a} \rangle ^c$
$\tilde{a}^3\Sigma_u^+$ 1^3B_2	560	0.0	0.0	0.0
$\tilde{b}^3\Pi_u$ 1^3A_1	14401	0.0	0.0	0.0
$\tilde{b}^3\Pi_u$ 1^3B_1		0.0	0.0	0.0

^aThe symmetry labels are given both for the linear molecule (point group $D_{\infty h}$), and for the bent molecule (point group C_{2v}).

^bMRCISD values obtained using SA-CASSCF wavefunctions computed by averaging 3 singlet and 3 triplet states (relative to the $\tilde{X}^1\Sigma_g^+$ state).

^cThe matrix elements (in a.u.) of the x , y , and z components of the dipole moment between the state in question and the corresponding lower state ($\tilde{X}^1\Sigma_g^+$ for singlet states and $\tilde{a}^3\Sigma_u^+$ for triplet states) calculated at the state-average CAS-MRCISD level of theory. The y -axis lies along the molecular axis.

Acknowledgements

B. O. gratefully acknowledges the financial support of the Ministry of Education, Science and Technological Development of the Republic of Serbia (Contract No. 172001). The work of P. J. is supported in part by the Deutsche Forschungsgemeinschaft and the Fonds der Chemischen Industrie. P. R. B. is grateful to Massey University for hospitality.

Table 3

Vertical singlet and triplet emission energies ΔE_{vert} (in cm^{-1}) of the lowest singlet and triplet excited states of BaOBa, calculated at the state-average CAS-MRCISD+ Q level of theory. The calculations were carried out at the equilibrium geometries of the corresponding excited states.

Singlet states							
State Φ^a	$r(\text{Ba-O})$	$\angle(\text{BaOBa})$	ΔE_{vert}^b	$ \langle\Phi \mu_x \tilde{X}\rangle ^c$	$\langle\Phi \mu_y \tilde{X}\rangle ^c$	$ \langle\Phi \mu_z \tilde{X}\rangle ^c$	
$\tilde{X}^1\Sigma_g^+$ (1^1A_1)	2.201 Å	180°	0	0.0	0.0	0.0	
$(\tilde{A}^1\Sigma_u^+)$ 1^1B_2	2.191 Å	149°	10934	0.0	3.60	0.0	
$\tilde{B}^1\Sigma_g^+$ (2^1A_1)	2.198 Å	180°	12342	0.0	0.0	0.0	
Triplet states							
State Φ^a	$r(\text{Ba-O})$	$\angle(\text{BaOBa})$	ΔE_{vert}^b	$ \langle\Phi \mu_x \tilde{a}\rangle ^c$	$ \langle\Phi \mu_y \tilde{a}\rangle ^c$	$ \langle\Phi \mu_z \tilde{a}\rangle ^c$	
$\tilde{a}^3\Sigma_u^+$ (1^3B_2)	2.201 Å	180°	0	0.0	0.0	0.0	
$(\tilde{b}^3\Pi_u)$ 1^3A_1	2.192 Å	153°	13749	0.0	1.62	0.0	
$\tilde{b}^3\Pi_u$ (1^3B_1)	2.184 Å	180°	13646	0.0	0.0	0.0	

^aThe symmetry labels are given both for the linear molecule (point group $D_{\infty h}$), and for the bent molecule (point group C_{2v}).

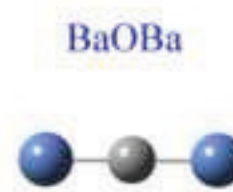
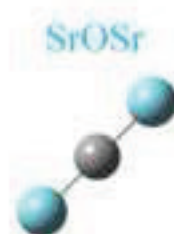
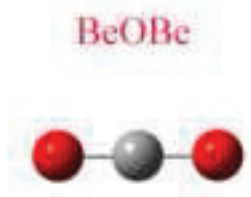
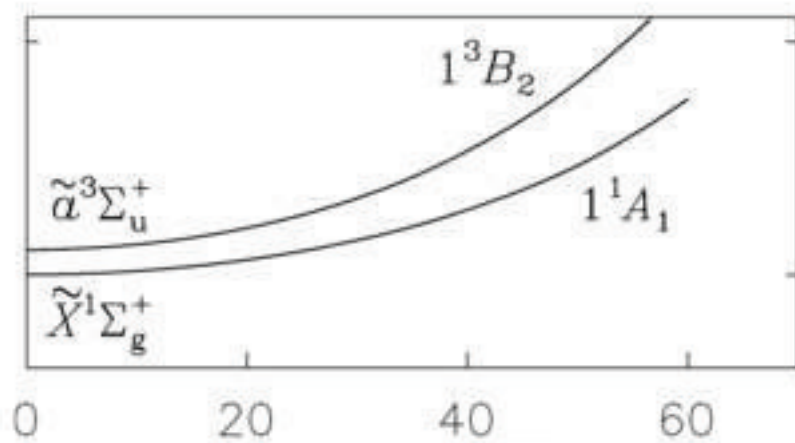
^bMRCISD values obtained using SA-CASSCF wavefunctions computed by averaging 3 singlet and 3 triplet states (relative to $\tilde{X}^1\Sigma_g^+$ for singlet states and to $\tilde{a}^3\Sigma_u^+$ for triplet states)

^cThe matrix elements (in a.u.) of the x , y , and z components of the dipole moment between the state in question and the corresponding lower state ($\tilde{X}^1\Sigma_g^+$ for singlet states and $\tilde{a}^3\Sigma_u^+$ for triplet states) calculated at the state-average CAS-MRCISD level of theory. The y -axis lies along the molecular axis.

References

- [1] B. Ostojić, P. Jensen, P. Schwerdtfeger, B. Assadollahzadeh, P. R. Bunker, *J. Mol. Spectrosc.* 263 (2010) 21-26.
- [2] B. Ostojić, P. R. Bunker, P. Schwerdtfeger, B. Assadollahzadeh, P. Jensen, *Phys. Chem. Chem. Phys.* 13 (2011) 7546-7553.
- [3] B. Ostojić, P. R. Bunker, P. Schwerdtfeger, A. Gertych, P. Jensen, *J. Mol. Struct.* 1023 (2012) 101-107.
- [4] B. Ostojić, P. Jensen, P. Schwerdtfeger, P. R. Bunker, *J. Phys. Chem.* 117 (2013) 9370-9379.
- [5] J.-P. Uzan, *Rev. Mod. Phys.* 75 (2003) 403-455.
- [6] P. Jansen, H. L. Bethlem, W. Ubachs, *J. Phys. Chem.* 140 (2013) 010901/1-13.
- [7] K. Beloy, A. W. Hauser, A. Borschevsky, V. V. Flambaum, P. Schwerdtfeger, *Phys. Rev. A* 84 (2011) 062114/1-4.
- [8] J. B. West, H. M. Poland, *J. Chem. Phys.* 66 (1977) 2139-2141.
- [9] S. A. Edelstein, B. E. Perry, D. J. Eckstrom, T. F. Gallagher, *Chem. Phys. Lett.* 49 (1977) 293-294.
- [10] C. Gée, M. A. Gaveau, J. M. Mestdagh, M. Osborne, O. Sublemontier, J. P. Visticot, *J. Phys. Chem.* 100 (1996) 13421-13427.
- [11] T. A. Isaev, S. Hoekstra, R. Berger, *Phys. Rev. A* 82 (2010) 052521/1-5.
- [12] M. N. Portela, J. E. van den Berg, H. Bekker, O. Böll, E. A. Dijck, G. S. Giri, S. Hoekstra, K. Jungmann, A. Mohanty, C. J. G. Onderwater, B. Santra, S. Schlessler, R. G. E. Timmermanns, O. O. Versolato, L. W. Wansbeek, L. Willmann, H. W. Wilschut, *Hyperfine Interact* 214 (2013) 157-162.
- [13] H.-J. Werner, P. J. Knowles, *J. Chem. Phys.* 82 (1985) 5053-5063.
- [14] P. J. Knowles, H.-J. Werner, *Chem. Phys. Lett.* 115 (1985) 259-267.
- [15] H.-J. Werner, P. J. Knowles, *J. Chem. Phys.* 89 (1988) 5803-5814.
- [16] P. J. Knowles, H.-J. Werner, *Chem. Phys. Lett.* 145 (1988) 514-522.
- [17] P. J. Knowles, H.-J. Werner, *Theor. Chim. Acta* 84 (1992) 95-103.
- [18] A. I. Boldyrev, I. L. Shamovsky, P. v. R. Schleyer, *J. Am. Chem. Soc.* 114 (1992) 6469-6475.
- [19] I. S. Lim, H. Stoll, P. Schwerdtfeger, *J. Chem. Phys.* 124 (2006) 034107/1-9.
- [20] S. R. Langhoff, E. R. Davidson, *Int. J. Quant. Chem.* 8 (1974) 61-72.

- [21] H.-J. Werner, P. J. Knowles, G. Knizia, F. R. Manby, M. Schütz, P. Celani, T. Korona, R. Lindh, A. Mitrushenkov, G. Rauhut, K. R. Shamasundar, T. B. Adler, R. D. Amos, A. Bernhardsson, A. Berning, D. L. Cooper, M. J. O. Deegan, A. J. Dobbyn, F. Eckert, E. Goll, C. Hampel, A. Hesselmann, G. Hetzer, T. Hrenar, G. Jansen, C. Köppl, Y. Liu, A. W. Lloyd, R. A. Mata, A. J. May, S. J. McNicholas, W. Meyer, M. E. Mura, A. Nicklass, D. P. O'Neill, P. Palmieri, K. Pflüger, R. Pitzer, M. Reiher, T. Shiozaki, H. Stoll, A. J. Stone, R. Tarroni, T. Thorsteinsson, M. Wang, and A. Wolf, MOLPRO, version 2010.1, a package of *ab initio* programs. See <http://www.molpro.net>.
- [22] Segmented Gaussian Basis Set, Quantum chemistry group, Sapporo, Japan. See <http://setani.sci.hokudai.ac.jp/sapporo/Welcome.do>
- [23] P. Celani, H.-J. Werner, J. Chem. Phys. 112 (2000) 5546-5557.
- [24] M. Reiher and A. Wolf, J. Chem. Phys. 121 (2004) 2037-2047.
- [25] M. Reiher and A. Wolf, J. Chem. Phys. 121 (2004) 10945-10956.
- [26] A. Wolf, M. Reiher, and B. A. Hess, J. Chem. Phys. 117 (2002) 9215-9226.
- [27] T. Helgaker, W. Klopper, H. Koch, J. Noga, J. Chem. Phys. 106 (1997) 9639-9646.
- [28] A. Halkier, T. Helgaker, P. Jørgensen, W. Klopper, H. Koch, J. Olsen, A. K. Wilson, Chem. Phys. Lett. 286 (1998) 243-252.
- [29] C. E. Moore, *Atomic Energy Levels*, (t) N-a.l. Bur. Stand. (U.S.) Circ. 467, Vol. III (1958); reprinted as Natl. Stand. Ref. Data. Ser., Natl. Bur. Stand. (U.S.) 35 (1971).
- [30] I. Lim, P. Schwerdtfeger, Phys. Rev. A 70 (2004) 062501/1-13.



ACCEPTED

- Theoretical study of electron structure in Group 2 M_2O hypermetallic oxides
- Focus on singlet-triplet interaction and singlet-triplet splittings
- *ab initio* calculation of 3D potential energy surfaces for BaOBa and RaORa
- Oxides have linear $\tilde{X}^1\Sigma_g^+$ ground electronic state and very low lying $\tilde{a}^3\Sigma_u^+$ state
- MgOMg has largest singlet-triplet splitting and does not fit into the overall trend

ACCEPTED MANUSCRIPT